EFFECT OF THE INLET OPENING ON MIXED CONVECTION INSIDE A 3-D VENTILATED CAVITY

by

Hicham DOGHMI*, Btissam ABOURIDA, Lahoucin BELARCHE, Mohamed SANNAD, and Meriem OUZAOUIT

National School of Applied Sciences, Ibn Zohr University, Agadir, Morocco

Original scientific paper
https://doi.org/10.2298/TSCI170126121D

Mixed convection heat transfer in a 3-D ventilated cavity is studied numerically using finite volume method. The results are presented in terms of streamlines, temperature distribution, velocity fields, and average Nusselt number for different combinations of thermal and geometrical controlling parameters, namely, Reynolds number, Re = 100, Richardson number (0.01 ≤ Ri ≤ 10), relative height of the openings (B = h/L = 1/8) and relative width (0.5 ≤ A = w/L ≤ 1). The obtained results show that the flow intensity and the heat transfer rate can be significantly improved by an optimal choice of the mentioned parameters.

Key words: *mixed convection, ventilated cavity, heat transfer, inlet opening, 3-D, numerical simulation*

Introduction

Mixed convection in ventilated cavities has been the subject of extensive research for many years due to the important coupling of the fluid flow and energy transport in this case. In fact, this phenomenon is involved in many engineering applications such as cooling of the electronic components, thermal design of buildings, furnace design, air conditioning, air-cooling, nuclear reactors, and others. This practical interest explains the existence of various studies considering this subject.

Hence, Papanicolaou and Jaluria [1, 2] studied numerically the mixed convection in a rectangular enclosure with a unique heat source and inlet and outlet openings placed in the vertical walls. For a fixed aspect ratio, Reynolds number and Grashof number were varied for various locations of the heat source and the outlet opening. The cooling rate was found to be higher when the outlet flow opening was located near the bottom of the vertical wall. A similar situation has been studied by Hsu *et al.* [3] with a partially dividing enclosure with a conducting baffle in two different orientations. They found that the higher heat transfer rate dissipated from the source is maximum when the outflow opening is placed at the lower part of the vertical wall, and a better cooling system was designed by placing the heat source close to the cold inlet stream. Rahman *et al.* [4] conducted a numerical study of the effects of Reynolds and Prandtl numbers on mixed convective flow and heat transfer characteristics in a ventilated cavity in the presence of a heat-generating solid circular obstacle placed at the center. They concluded that the average Nusselt number at the heated surface for different values of Richardson number can be increased with the increasing of the Reynolds and Prandtl numbers.

* Corresponding author, e-mail: hicham.gte@gmail.com

Aminossadati and Ghasemi [5] have investigated the mixed convection in an open cavity for three different locations of a heat source (left, right, and bottom) and different aspect ratio. The effect of these parameters on the fluid flow and heat transfer has been examined for different Richardson numbers. They found that at a fixed Richardson number, all three different heating modes corresponded to noticeable improvements in the heat transfer mechanism as the cavity aspect ratio increased. An experimental investigation on mixed convection in open cavities with heated inflow wall was carried out by Manca *et al.* [6]. The principal results showed that the maximum dimensional temperature decreases as the Reynolds and the Richardson numbers are decreasing. They observed also, for Re = 1000, a parallel forced flow motion in the channel and a re-circulation flow inside the cavity.

Selimefendigil and Oztop [7] analyzed numerically the effect of the adiabatic thin fin on the mixed convection performance in 2-D square cavity with two ventilation ports. El-Maghlany *et al.* [8] examined the natural convection heat transfer behavior and entropy generation inside an infinite square cavity. Teamah and El-Maghlany [9] studied numerically the natural convection in a square cavity filled with nanofluids in the presence of magnetic field and uniform heat generation/absorption.

Numerical studies of the double-diffusive mixed convection heat transfer in a lid-driven square cavity under the combined buoyancy effects of thermal and mass diffusion was reported in [10-14].

The references [15-18] included numerically the radiative exchange effects among the cavity walls. The results showed that the combination of the mixed convection and radiation could be important, even though the radiation effect leads to a better homogenization of the temperature inside the cavity by reducing the cold zone at the entrance region.

Raji and Hasnaoui [19-21] conducted a numerical study of mixed convection heat transfer in a ventilated cavity with a laminar cold jet and heated with a constant heat flux. The obtained results show the presence of a maximum interaction between natural and forced convection occurs for couples (Ra, Re) and the existence of different flow regimes, which can be divided into regions corresponding to the dominance of the forced convection or to the mixed convection regime and the limits between both regimes, were determined and correlated *vs.* Rayleigh number. The BT configuration where the fluid leaves the cavity via the top, was found to be more useful to reduce the mean temperatures inside the cavity for Re < 1000.

Mixed convection in an air-cooled cavity was studied numerically by Omri and Nasrallah [22] for two different positions of the inlet and outlet openings on the sidewalls of the cavity. The results presented show that the clearance of the heat is more effective when the air is injected from the bottom of the hot wall. Singh and Sharif [23] studied numerically the mixed convective cooling in a rectangular cavity deferentially heated by considering six placements of the inlet and exit ports. Their results showed that maximum cooling effectiveness is achieved if the inlet is kept near the bottom of the cold wall and the outlet is located near the top of the hot wall.

We can notice that the majority of the previous works considers the case of 2-D flow and heat transfer while very few studies have been conducted for 3-D numerical simulation. Therefore, mixed convective heat transfer in an open 3-D cavity with a heated block was studied by Kanna *et al.* [24], by using fluent CFD code. They analyzed the flow structure, heat transfer characteristics and the complex interaction between the induced stream flow at ambient temperature and the buoyancy-induced flow from the walls of the heated source. The 3-D mixed convection in partially opened cavities with internal heat sources are investigated numerically by Fontana *et al.* [25]. Their results show the existence of two different processes

controlling the formation of re-circulation inside the cavity: hydrodynamic re-circulation and thermal re-circulation. Also, they showed a strong 3-D nature of the flow inside the cavity, indicating that a simplified 2-D model is not able to capture some important aspects of the system behavior. Stiriba *et al.* [26] investigated numerically the mixed convective flow over a 3-D cavity placed at the bottom of a horizontal channel. They found that for both high Reynolds and Grashof numbers, the mixed convection effects come into play, push the recirculating zone further upstream and the flow becomes unsteady with Kelvin-Helmholtz instabilities at the shear layer while the Nusselt number increases for Re = 1000 and Gr = 107. Moraga and Lopez [27] compared numerically the mixed convection in a 2-D and 3-D air-cooled cavity. They found that the 2-D model is only able to predict values for the global Nusselt number that are similar to the more accurate values obtained with the 3-D models. When Re < 50, major differences between the global Nusselt numbers calculated from the 2-D and the 3-D models. Hence, the 3-D model must be used to capture the fluid mechanics for Ri = 10 when $10 \leq \mathrm{Re} \leq 250$, and to calculate the global Nusselt number when Re = 500 for Ri < 1.

Hence, the literature review shows that the 3-D approach gives a better modelization of the fluid flow and heat transfer within the cavity. This explains the choice of our present physical model, which intended to investigate numerically the effects of conjugated Richardson numbers and geometrical parameters on the thermal transport and fluid flow phenomena in the considered enclosure.

Problem formulation

The studied configuration and the co-ordinates are presented in fig. 1. It consists of a cubical 3-D ventilated cavity ($H = L = W$), with an inlet opening of a rectangular cross-section of relative height $B = h/L$ and a relative width ranging between $0.5 \leq A = w/L \leq 1$. The inlet opening is located on the top of the left vertical wall, allowing air flow to get in, at a uniform velocity U_{in} and ambient temperature T_c. The two sections on each side of the inlet opening are adiabatic. Underneath the opening, the remaining part of the wall is heated with a uniform temperature T_h. An outlet opening with a relative height $B = h/L$ is placed at the bottom of the right vertical wall, which is maintained at cold temperature T_c.

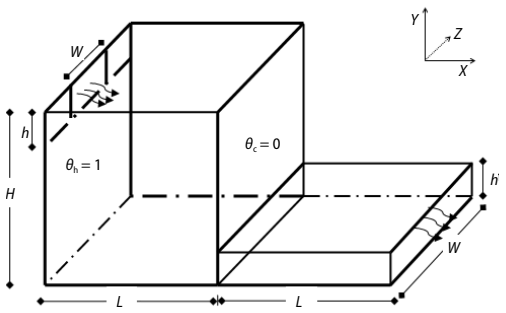

Figure 1. Studied configuration and co-ordinates

A channel with the same cross-section is placed at the opening to extend the cavity and makes possible the use of developed boundary conditions for the fluid flow and heat transfer at the outlet. Many tests have been done in order to check the influence of the channel length on the outlet boundary conditions. The average Nusselt number and velocity profiles maximum variation between the length equal to $2L$ and without extended section is less than 4%. Finally, a length of L has been adopted as it gives a compromise between the results accuracy and the computational time. The other four walls of the cavity are maintained adiabatic.

The considered cooling fluid is air, which has a Prandtl number of 0.71 and is assumed laminar and incompressible with negligible viscous dissipation. All the thermo-physical properties of the fluid are assumed constant except the density, giving rise to the buoyancy forces (Boussinesq approximation).

The governing equations for the 3-D laminar incompressible fluid are expressed in the following dimensionless form:

$$\frac{\partial U}{\partial X}+\frac{\partial V}{\partial Y}+\frac{\partial W}{\partial Z}=0 \tag{1}$$

$$U\frac{\partial U}{\partial X}+V\frac{\partial U}{\partial Y}+W\frac{\partial U}{\partial Z}=-\frac{\partial P}{\partial X}+\frac{1}{\mathrm{Re}}\left(\frac{\partial^2 U}{\partial X^2}+\frac{\partial^2 U}{\partial Y^2}+\frac{\partial^2 U}{\partial Z^2}\right) \tag{2}$$

$$U\frac{\partial V}{\partial X}+V\frac{\partial V}{\partial Y}+W\frac{\partial V}{\partial Z}=-\frac{\partial P}{\partial Y}+\frac{1}{\mathrm{Re}}\left(\frac{\partial^2 V}{\partial X^2}+\frac{\partial^2 V}{\partial Y^2}+\frac{\partial^2 V}{\partial Z^2}\right)+\frac{\mathrm{Gr}}{\mathrm{Re}^2}\theta \tag{3}$$

$$U\frac{\partial W}{\partial X}+V\frac{\partial W}{\partial Y}+W\frac{\partial W}{\partial Z}=-\frac{\partial P}{\partial Z}+\frac{1}{\mathrm{Re}}\left(\frac{\partial^2 W}{\partial X^2}+\frac{\partial^2 W}{\partial Y^2}+\frac{\partial^2 W}{\partial Z^2}\right) \tag{4}$$

$$U\frac{\partial \theta}{\partial X}+V\frac{\partial \theta}{\partial Y}+W\frac{\partial \theta}{\partial Z}=\frac{1}{\mathrm{Re}\,\mathrm{Pr}}\left(\frac{\partial^2 \theta}{\partial X^2}+\frac{\partial^2 \theta}{\partial Y^2}+\frac{\partial^2 \theta}{\partial Z^2}\right) \tag{5}$$

The non-dimensional variables are defined:

$$X=\frac{x}{L},\quad Y=\frac{y}{L},\quad Z=\frac{z}{L} \tag{6}$$

$$U=\frac{u}{u_{\mathrm{in}}},\quad V=\frac{v}{u_{\mathrm{in}}},\quad W=\frac{w}{u_{\mathrm{in}}},\quad P=\frac{p-p_0}{\rho_0 u_{\mathrm{in}}^2},\quad \theta=\frac{T-T_{\mathrm{c}}}{T_{\mathrm{h}}-T_{\mathrm{c}}} \tag{7}$$

where p_0 and ρ_0 are, respectively, the reference pressure and density. T_{h} is the temperature at the heated surface, T_{c} the temperature at the cooled surface, and p the pressure.

In the previous equations, the parameters Pr, Gr and Re denote the Prandtl number, Grashof number, and the Reynold number, respectively. These parameters are defined:

$$\mathrm{Re}=\frac{Lu_{\mathrm{in}}}{\nu},\quad \mathrm{Gr}=\frac{g\beta L^3(T_{\mathrm{h}}-T_{\mathrm{c}})}{\nu^2},\quad \mathrm{Ri}=\frac{\mathrm{Gr}}{\mathrm{Re}^2},\quad \mathrm{Pr}=\frac{\nu}{\alpha} \tag{8}$$

where β, ν, and α are the thermal expansion coefficient, the kinematic viscosity and the thermal diffusivity, respectively.

The boundary conditions, associated to the problem are:

- $U = V = W = 0$ on the rigid walls of the enclosure,
- $U = 1$, $V = W = 0$, $\theta_{\mathrm{c}} = 0$ at the inlet,
- $\theta_{\mathrm{h}} = 1$ on the left vertical heated wall,
- $\theta_{\mathrm{c}} = 0$ on the right vertical cooled wall,
- $\partial\theta/\partial n = 0$ on other vertical and horizontal walls and the right and left sections near the opening (n is the normal direction to the considered wall), and
- $\partial U/\partial X = 0$, $\partial\theta/\partial X = 0$, $V = W = 0$ at the outlet.

The local Nusselt number and the average Nusselt number characterizing the heat transfer at the heated and cooled walls are, respectively, defined:

$$\mathrm{Nu}_{\mathrm{local}}(Y,Z)=\frac{\partial\theta}{\partial X}\quad \text{at}\quad X=0\quad \text{or}\quad X=1 \tag{9}$$

$$\mathrm{Nu_h} = \int_0^{1-B}\int_0^1 \mathrm{Nu}(Y,Z)\mathrm{d}Y\mathrm{d}Z \tag{10}$$

$$\mathrm{Nu_c} = \int_B^1\int_0^1 \mathrm{Nu}(Y,Z)\mathrm{d}Y\mathrm{d}Z \tag{11}$$

Numerical method

The described mathematical model was solved by the home-developed FORTRAN code. The incompressible Navier-Stokes and energy equations are discretized by the finite volume method developed by Patankar [28] adopting the power law scheme for the convective terms. The SIMPLEC algorithm is used to couple momentum and continuity equations. The discretized equations are iteratively solved using an alternating direction implicit (ADI) scheme. The system of algebraic equations is solved iteratively by means of the Thomas algorithm.

Convergence of the numerical code is established according to the following criterion:

$$\sum_{i,j,k=1}^{i\max,j\max,k\max} \frac{\left|\phi_{i,j,k}^{n+1} - \phi_{i,j,k}^{n}\right|}{\left|\phi_{i,j,k}^{n}\right|} \le 10^{-4} \tag{12}$$

where ϕ represents a dependent variable U, V, W, T, and P, the indices i, j, and k indicate the grid positions, and n represents the iteration number.

Code and grid size validation

The preliminary tests were used to check the grid independency of the solution using different uniform grid sizes. The grid 91 × 71 × 71 was estimated to be appropriate for the present study since it permits a good compromise between the computational cost and the accuracy of the obtained results. In addition, the maximum deviation remains within 1.5% when the grid was refined to 101 × 81 × 81.

The obtained results are compared with the existing 2-D and 3-D studies of Omri and Nasrallah [22] and Moraga and Lopez [27], in terms of velocity profiles and temperature distribution, for different sets of the governing parameters. Figures 2(a) and 2(b) show U and V velocity components at the vertical and horizontal midlines, respectively, for Re = 10 and

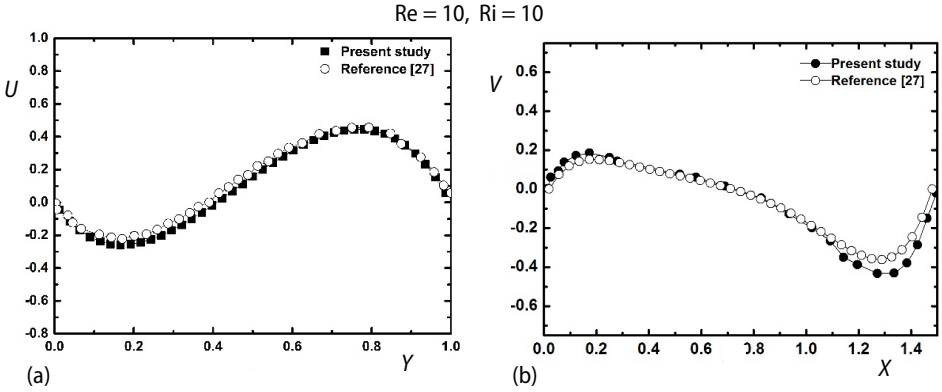

Figure 2. (a) U velocity component at $X = 0.75$, $Z = 0.5$, and (b) V velocity component at $Y = 0.5$, $Z = 0.5$

Ri = 10. It can be seen from this comparison that there is a good agreement between the present results and those presented by Moraga and Lopez [27].

Figure 3 shows the isotherms for 2-D and 3-D models for Re = 10, and Ri = 0.1, 10 at Z = 0.5.

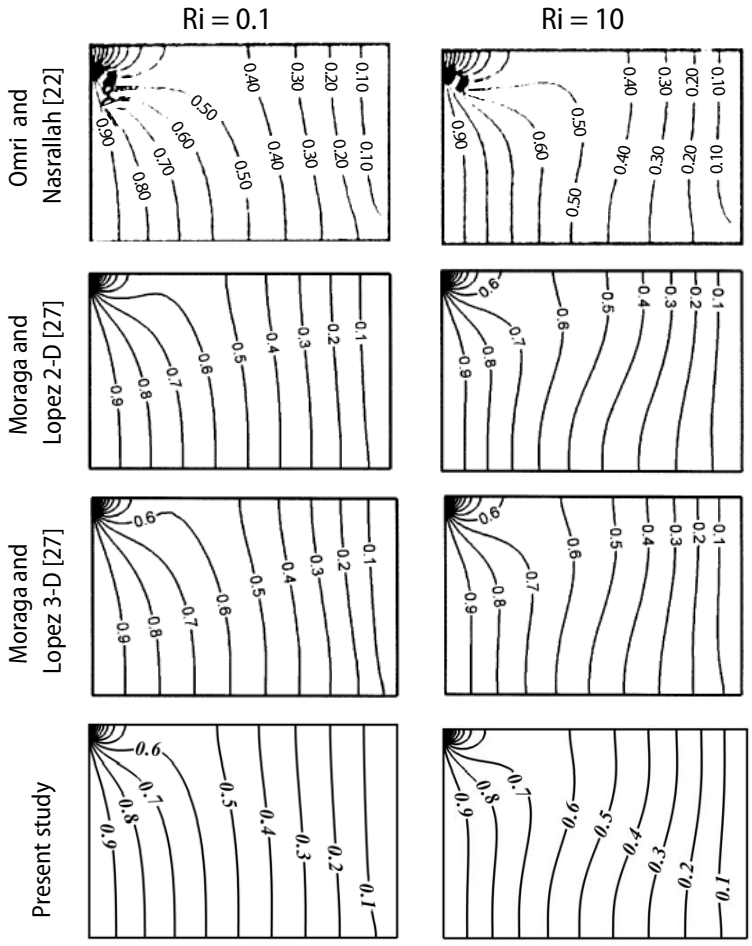

Figure 3. Comparison between the isotherm obtained at the middle plane $Z = 0.5$ and those of Omri and Nasrallah [22] and Moraga and Lopez [27]

Results and discussion

In this paper, we present the conjugated effects of Richardson number and geometrical parameter A on the thermal transfer and fluid flow phenomena within the 3-D ventilated cavity. The numerical computations are conducted over a wide range of Richardson number ($0.01 \leq \mathrm{Ri} \leq 10$) and the relative width of the inlet opening $0.5 \leq A \leq 1$. The Reynolds number Re is maintained equal to 100, which correspond to a laminar regime. The relative height of the inlet opening B and the Prandtl number are fixed to 1/8 and 0.71, respectively. The relative height and width of the outlet opening are maintained constant at $B = 1/8$ and $A = 1$, respectively.

Effect of Richardson numbers

In this section, we study the effect of Richardson number on 3-D flow structure and temperature distribution within the cavity. The inlet opening relative width was kept at a constant value $A = 0.5$.

To give an overview of the cavity, fig.4 illustrates the 3-D streamlines and isotherms, while fig. 5 is representing the flow and temperature distribution in different plans ($Z = 0.1$, 0.25, and 0.5). In fact, the analysis of the isotherms and streamlines in different planes ($0 \leq Z \leq 1$) shows a perfect symmetry with respect to the plane $Z = 0.5$. This is due to the geometrical symmetry and adopted thermal boundary conditions.

Figures 4 and 5, indicate that the streamlines and isotherms are highly affected by the changing of the Richardson number. For Ri < 1, figs. 4(a) and 5(a), the isolines show the presence of a cell clockwise rotating inside the cavity and located under the opened lines of the forced flow. These ones are directed to the outlet due to the dominance of inertia forces. We also noticed the presence of two symmetrical small vortexes located at the top of the cavity.

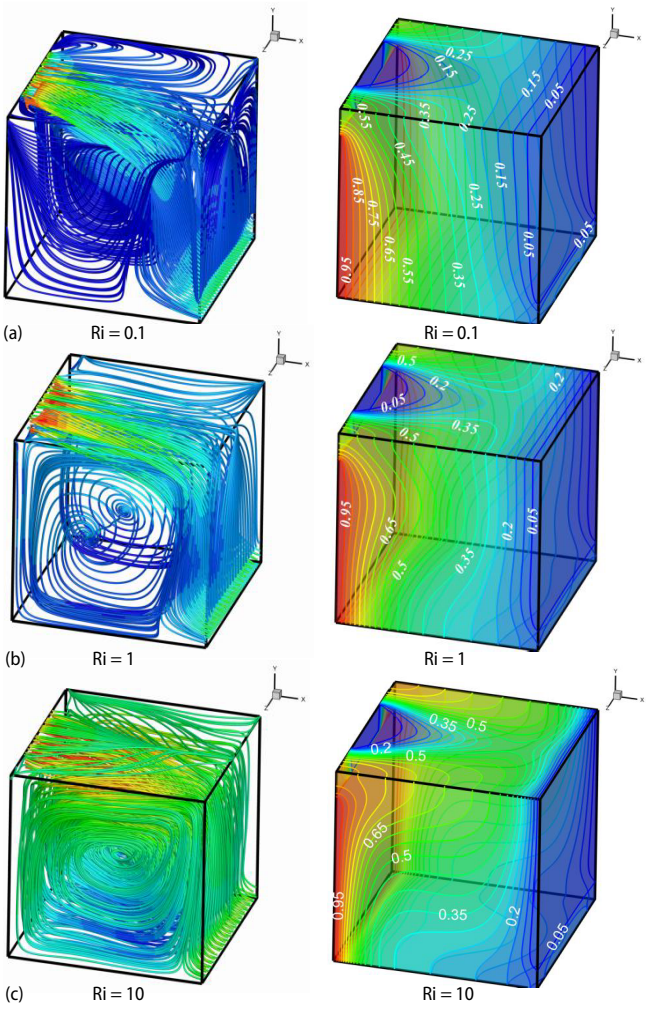

Figure 4. The 3-D streamlines and isotherm lines at different values of Ri (*for color image see journal web site*)

As the Richardson number increases to Ri = 1, a change in the flow structure and the isotherms is then observed, figs. 4(b) and 5(b). The complex structure in the upper part of the cavity disappears and the balance between inertia and buoyancy forces increases the size and the intensity of the convective cell. The corresponding isotherms are condensed near the heated and the cold wall of the cavity due to the imposed boundary conditions, and the temperature distribution is nonlinear in the remaining parts of the cavity.

By increasing progressively Ri from 1 to 10, figs. 4(c) and 5(c), the role of free convection in the cavity becomes more significant and consequently the size of the vortex increases so it occupies almost the whole domain. This intensification of the flow improved the heat exchange between the active walls of the cavity and the incoming flow characterized by a visible tightening of the isotherms at the vicinity of these walls as we observed from the analysis of the isotherms.

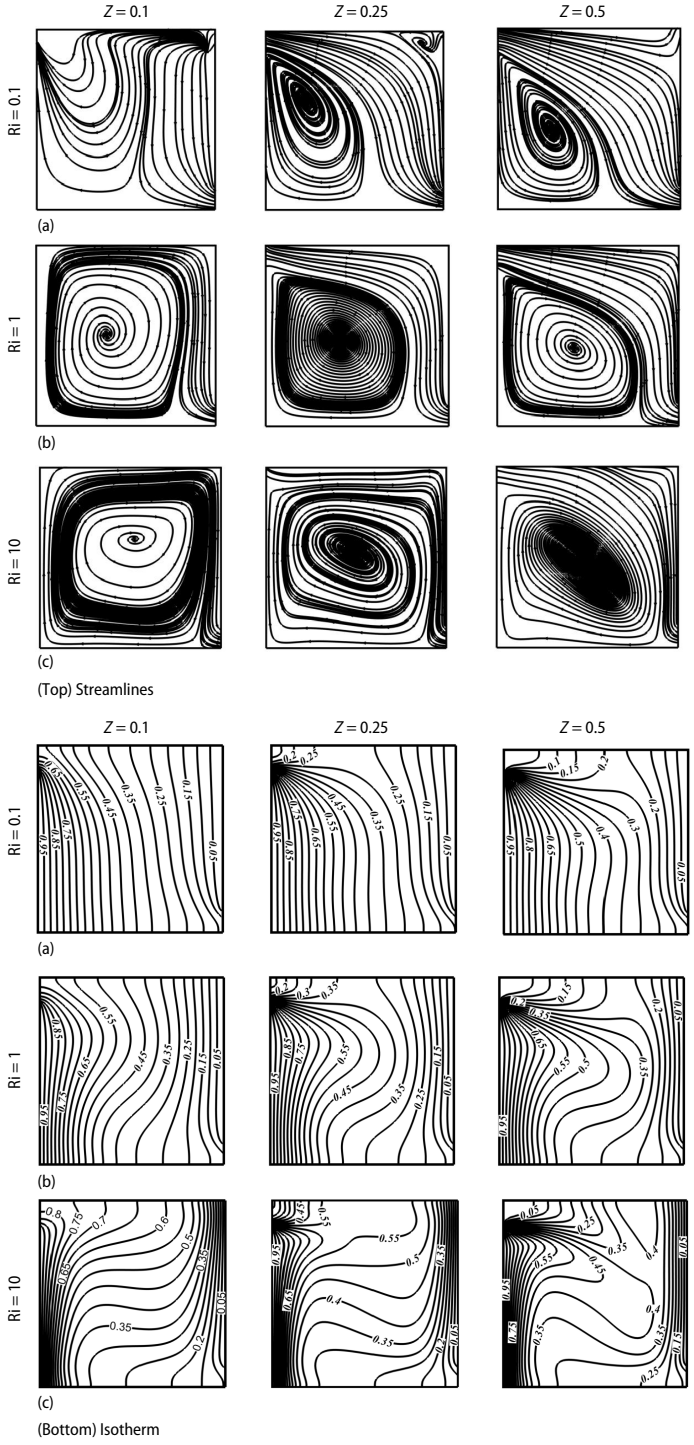

Figure 5. Streamlines (top) and isotherm lines (bottom) at different Z-planes for: (a) Ri = 0.1, (b) Ri = 1, and (c) Ri = 10

Effect of the opening width

To figure out the impact of the inlet opening relative width A on the flow pattern and heat transfer, we represent in fig. 6 the streamlines and isotherms for Ri = 5 and different values of A at Z central plan ($Z = 0.5$).

When $A = 0.5$, fig. 6(a) shows that the open lines related to the externally forced flow are affected by the heated surface under the opening. The small inlet cross-section leads to an acceleration of the cold forced flow through the cavity along the cold wall to the exit. On the other hand, the internal fluid is reversed toward the hot zone forming weakened buoyancy-driven circulating flow, which does not mix well with the incoming air jet. The examination of the isotherm lines shows an improvement in the exchange at the cold wall of the cavity.

By increasing the relative width to $A = 0.75$, fig. 6(b) the size of the convective cell increase and the acceleration of the external forced flow is slightly decreased which give the time to the buoyancy effect along the hot wall to acts favorably with the ambient fluid, the mixed convection is achieved. Some enhancement of heat transfer occurs from the heating zone to the cold vertical wall.

More increase of A ($A = 1$), leads to an intensification of the flow, fig. 6(c). Hence, the convective cell,

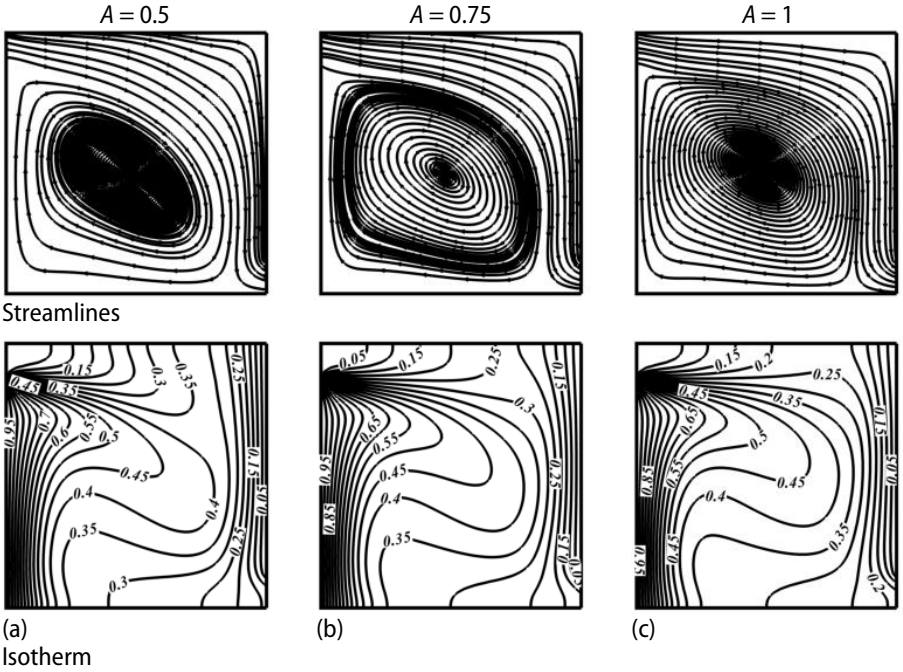

Figure 6. Streamlines (top) and isotherm lines (bottom) at $Z = 0.5$ for Ri = 5: (a) $A = 0.5$, (b) $A = 0.75$, and (c) $A = 1$

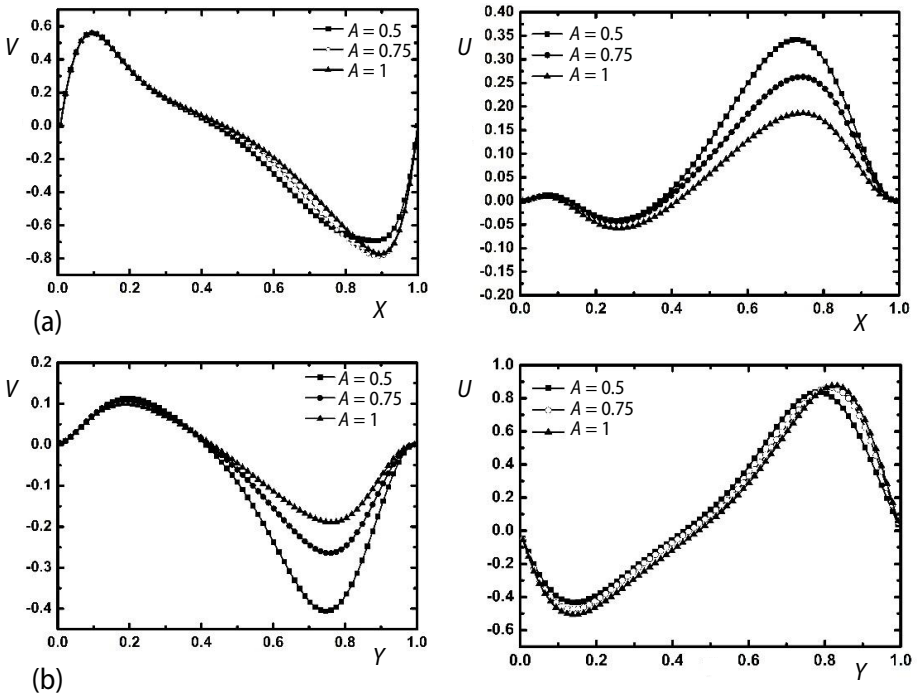

Figure 7. Profiles of dimensionless vertical V and horizontal U velocities along: (a) an horizontal midline at $Y = 0.5$, $Z = 0.5$, (b) a vertical midline at $X = 0.5$, $Z = 0.5$, for various values of A

under the external flow open lines, is occupying most of the cavity and rotating in the clockwise direction. This leads to more favorable heat transfer shown by a better stratification of the temperature. In fact, the increase of the opening relative width precipitates the establishment of the mixed convection mode by supporting the formation and intensification of natural convection cell.

Figure 7(a) shows the V-velocity profile along the horizontal midline $Y = 0.5$ and $Z = 0.5$. The vertical velocity component V increases from the hot wall and reaches a maximum. This is due to the combined effects of the inertia force and thermal buoyancy in the vertical direction where the boundary layers become thinner. An abrupt decrease in the opposite direction is then encountered and V passes through a minimum value, meaning that the fluid is moving down near the cold wall. From this optimum value, the velocity increases until it becomes equal to zero at the right vertical wall. Figure 7(b) shows the U-velocity component along the vertical central line. The horizontal velocity U profile is negative (incoming cold flow), then increases until reaching maximum values (leaving heated flow). By increasing the inlet cross-section, the $U(Y)$ is slightly decreased in the core of the cavity and increase near the top wall, which reached a maximum value then tends toward zero. On the other hand, the vertical velocity $V(X)$ is almost independent of A at the left part of the cavity then increases with it (in absolute value) on the remaining part. This behavior is a consequence of the interaction between the incoming jet flow and the thermal buoyancy effect, which allows the installation of mixed convection.

The higher velocity profiles U in the main flow direction X are obtained by decreasing the width of the opening referring to the flow conservation. However, the maximum speed values are encountered in the range $X, Y > 0.4$, where the fluid is more accelerated in the jet direction along the cold wall through the cavity exit.

Heat transfer enhancement

The variations of the average Nusselt numbers, calculated on the hot and cold walls, are illustrated in figs. 8(a) and 8(b), respectively, *vs.* Richardson number and for different opening widths A. The Nusselt number increases with increasing Richardson numbers for all the considered opening widths A. This can be explained by the enhancement of thermal interaction between the natural convection flow and the incoming forced flow since the buoyancy effects become the dominant mode of the mixed convection transport. In addition, for a given number Ri, the increase of the opening width A enhances significantly the heat transfer on the hot wall. This is due to the increasing amount of the fluid coming through the inlet opening. In contrast,

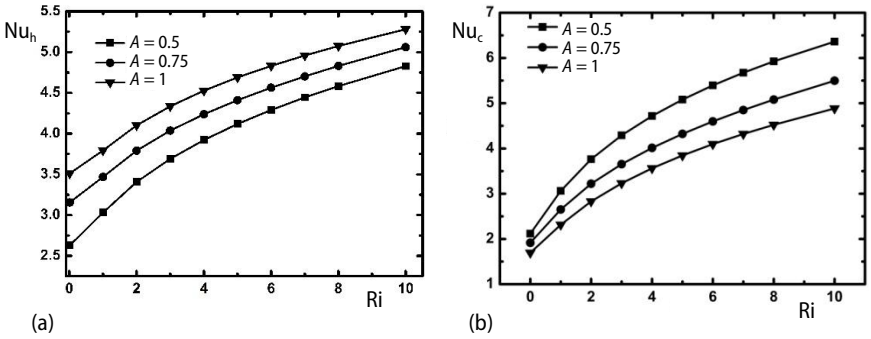

Figure 8. Average Nusselt number (a) at the hot wall Nu_h and (b) at the cold wall Nu_c as a function of Ri for $A = 0.5$, 0.75, and 1

the Nusselt number at the cold wall increases by decreasing A for a given value of Richardson number. The differences are more important when $Ri \geq 1$ and $Ri \geq 6$ for $A = 0.5$ and $A = 0.75$, respectively. In fact, the internal heated air rises fast (natural convection) and pushed by the incoming accelerated flow (forced convection) near the cold wall through the exit vicinity, which leads to a better stratification of the temperature at the cold wall.

Conclusions

Mixed convective heat transfer in 3-D ventilated cavity has been studied for different sets of the governing parameters (Richardson number and the opening cross-sections dimensions) and leads to the following conclusions.

- The forced convection dominates the flow transport mechanism when $Ri < 1$ resulting on a heat transfer dominated by conduction.
- The fluid flow consists of a big cell occupying almost the whole domain when $Ri > 1$; the role of free convection in the cavity becomes then more significant.
- The average Nusselt number at the active walls increases with increasing Richardson number.
- For fixed Richardson number, the Nusselt number increases at the hot wall and decreases at the cold wall, when the A is increased.
- The heat exchange at the cold wall is more important than the one at the heated wall ($Nu_c > Nu_h$) when $Ri \geq 1$ and $Ri \geq 6$ for $A = 0.5$ and $A = 0.75$, respectively.

Nomenclature

A – relative width of the inlet opening, (= w/L), [–]
B – relative height of the openings, (= h/L), [–]
Gr – Grashof number, [–]
g – acceleration due to gravity, [ms^{-2}]
H – height of the cavity, [m]
h – height of the openings, [m]
L – length of the cavity, [m]
Nu – Nusselt number, [–]
P – dimensionless pressure, [–]
Pr – Prandtl number, [–]
Ra – Rayleigh number, [–]
Re – Reynolds number, [–]
Ri – Richardson number, [–]
U, V, W – dimensionless velocity components, [–]
u, v, w – dimensional velocities, [ms^{-1}]
W – width of the cavity, [m]
X, Y, Z – dimensionless cartesian co-ordinates, [–]
x, y, z – dimensional co-ordinates, [m]

Greek symbols

α – thermal diffusivity, [m^{2}s^{-1}]
β – volumetric thermal expansion coefficient, [K^{-1}]
θ – non-dimensional temperature, [–]
ν – kinematic viscosity, [m^{2}s^{-1}]
ρ – density, [kgm^{-3}]

Subscripts

c – cold
h – hot
i, j, k – node position
in – inlet

References

[1] Papanicolaou, E., Jaluria, Y., Mixed Convection from an Isolated Heat Source in a Rectangular Enclosure, *Numerical Heat Transfer*, *18* (1991), 4, pp. 427-461
[2] Papanicolaou, E., Jaluria, Y., Mixed Convection from a Localized Heat Source in a Cavity with Conducting Walls: A Numerical Study, *Numerical Heat Transfer, Part A Applications*, *23* (1993), 4, pp. 463-484
[3] Hsu, T. H., *et al.*, Mixed Convection in a Partially Divided Rectangular Enclosure, *Numerical Heat Transfer, Part A Applications, 31* (1997), 6, pp. 655-683
[4] Rahman, M., *et al*, Effects of Reynolds and Prandtl Number on Mixed Convection in a Ventilated Cavity with a Heat-Generating Solid Circular Block, *Applied Mathematical Modelling*, *36* (2012), 5, pp. 2056-2066
[5] Aminossadati, S. M., Ghasemi, B., A Numerical Study of Mixed Convection in a Horizontal Channel with a Discrete Heat Source in an Open Cavity, *European Journal of Mechanics-B/Fluids, 28* (2009), 4, pp. 590-598

[6] Manca, O., *et al.,* Experimental Investigation of Mixed Convection in a Channel with an Open Cavity, *Experimental Heat Transfer*, *19* (2006), 1, pp. 53-68
[7] Selimefendigil, F., Oztop, H. F., Effects of an Adiabatic Fin on the Mixed Convection Heat Transfer in a Square Cavity with Two Ventilation Ports, *Thermal Science, 18* (2014), 2, pp. 377-389
[8] Teamah, M. A., El-Maghlany, W. M., Numerical Simulations of the Effect of an Isotropic Heat Field on the Entropy Generation Due to Natural Convection in a Square Cavity, *Energy Conversion and Management*, *85* (2014), Sept., pp. 333-342
[9] Teamah, M. A., El-Maghlany, W. M., Augmentation of Natural Convective Heat Transfer in Square Cavity by Utilizing Nanofluids in the Presence of Magnetic Field and Uniform Heat Generation/Absorption, *International Journal of Thermal Sciences*, *58* (2012), Aug., pp. 130-142
[10] Teamah, M. A., El-Maghlany, W. M., Numerical Simulation of Double-Diffusive Mixed Convective Flow in Rectangular Enclosure with Insulated Moving Lid, *International Journal of Thermal Sciences*, *49* (2010), 9, pp. 1625-1638
[11] Teamah, M. A., *et al*., Numerical Simulation of Double Diffusive Laminar Mixed Convection in Shallow Inclined Cavities with Moving Lid, *Alexandria Engineering Journal*, *52* (2013), 3, pp. 227-239
[12] Teamah, M. A., *et al*., Mixed Convection Heat Transfer in a Lid-Driven Square Cavity Completely Filled with Porous Material, *Int. J. Appl. Eng. Res., 10* (2015), pp. 28105-28128
[13] Rahman, M. M., *et al*., Unsteady Mixed Convection in a Porous Media Filled Lid-Driven Cavity Heated by a Semi-Circular Heaters, *Thermal Science*, *19* (2015), 5, pp. 1761-1768
[14] Pourmahmoud, N., *et al*., Numerical Comparison of Viscosity Models on Mixed Convection in Double Lid-Driven Cavity Utilized CuO-Water Nanofluid, *Thermal Science*, *20* (2016), 1, pp. 347-358
[15] Raji, A., Hasnaoui, M., Combined Mixed Convection and Radiation in Ventilated Cavities, *Engineering Computations*, *18* (2001), 7, pp. 922-949
[16] Bahlaoui, A., *et al.,* Height Partition Effect on Combined Mixed Convection and Surface Radiation in a Vented Rectangular Cavity, *Journal of Applied Fluid Mechanics*, *4* (2011), 1, pp. 89-96
[17] Bahlaoui, A*, et al.,* Coupling between Mixed Convection and Radiation in an Inclined Channel Locally Heated, *J. Mech. Eng.*, *55* (2004), pp. 45-57
[18] Bahlaoui, A., *et al.*, Mixed Convection Cooling Combined with Surface Radiation in a Partitioned Rectangular Cavity, *Energy Conversion and Management*, *50* (2009), 3, pp. 626-635
[19] Raji, A., Hasnaoui, M., Mixed Convection Heat Transfer in a Rectangular Cavity Ventilated and Heated from the Side, *Numerical Heat Transfer, Part A: Applications, 33* (1998), 5, pp. 533-548
[20] Raji, A., Hasnaoui, M., Correlations on Mixed Convection in Ventilated Cavities, *Revue Générale de Thermique, 37* (1998), 10, pp. 874-884
[21] Raji, A., Hasnaoui, M., Mixed Convection Heat Transfer in Ventilated Cavities with Opposing and Assisting Flows, *Engineering Computations*, *17* (2000), 5, pp. 556-572
[22] Omri, A., Nasrallah, S. B., Control Volume Finite Element Numerical Simulation of Mixed Convection in an Air-Cooled Cavity, *Numerical Heat Transfer: Part A: Applications*, *36* (1999), 6, pp. 615-637
[23] Singh, S., Sharif, M. A. R., Mixed Convective Cooling of a Rectangular Cavity with Inlet and Exit Openings on Differentially Heated Side Walls, *Numerical Heat Transfer: Part A: Applications*, *44* (2003), 3, pp. 233-253
[24] Kanna, P. R*., et al.*, Numerical Investigation of Mixed Convection Heat Transfer from Block Mounted on a Cavity, *Arabian Journal for Science and Engineering*, *39* (2014), 12, pp. 9187-9204
[25] Fontana, E., *et al.*, Numerical Analysis of Mixed Convection in Partially Open Cavities Heated from Below, *International Journal of Heat and Mass Transfer*, *81* (2015), pp. 829-845
[26] Stiriba, Y., *et al.*, A Numerical Study of Three-Dimensional Laminar Mixed Convection Past an Open Cavity, *International Journal of Heat and Mass Transfer*, *53* (2010), 21, pp. 4797-4808
[27] Moraga, N. O., Lopez, S. E., Numerical Simulation of Three-Dimensional Mixed Convection in an Air-Cooled Cavity, *Numerical Heat Transfer, Part A: Applications*, *45* (2004), 8, pp. 811-824
[28] Patankar, S. V., *Numerical Heat Transfer and Fluid Flow,* McGraw-Hill, New York, USA, 1980

Paper submitted: January 26, 2017
Paper revised: April 4, 2017
Paper accepted: April 20, 2017

© 2018 Society of Thermal Engineers of Serbia
Published by the Vinča Institute of Nuclear Sciences, Belgrade, Serbia.
This is an open access article distributed under the CC BY-NC-ND 4.0 terms and conditions